Title

Employing a Narrow-Band-Gap Mediator in Ternary Solar Cells for Enhanced Photovoltaic Performance

Journal

ACS Applied Materials & Interfaces, 12(14)

ISSN

1944-8244

Authors

Xiao, Liangang
Mao, Haiyan
Li, Zhengdong
et al.

Publication Date

2020-04-08

DOI

10.1021/acsami.9b23516

Peer reviewed

ACS APPLIED MATERIALS & INTERFACES

www.acsami.org

Research Article

Employing a Narrow-Band-Gap Mediator in Ternary Solar Cells for Enhanced Photovoltaic Performance

Liangang Xiao,[⊥] Haiyan Mao,[⊥] Zhengdong Li, Cong Yan, Jia Liu, Yidong Liu, Jeffrey A. Reimer, Yonggang Min,* and Yi Liu*

Cite This: *ACS Appl. Mater. Interfaces* 2020, 12, 16387−16393

Read Online

ACCESS | Metrics & More | Article Recommendations | Supporting Information

ABSTRACT: Ternary organic solar cells (OSCs) provide a convenient and effective means to further improve the power conversion efficiency (PCE) of binary ones via composition control. However, the role of the third component remains to be explored in specific binary systems. Herein, we report ternary blend solar cells by adding the narrow-band-gap donor PCE10 as the mediator into the PBDB-T:IDTT-T binary blend system. The extended absorption, efficient fluorescence resonance energy transfer, enhanced charge dissociation, and induced tighter molecular packing of the ternary blend films enhance the photovoltaic properties of devices and deliver a champion PCE of 10.73% with an impressively high open-circuit voltage (V_{OC}) of 1.03 V. Good miscibility and similar molecular packing behavior of the components guarantee the desired morphology in the ternary blend films, leading to solar cell devices with over 10% PCEs at a range of compositions. Our results suggest that ternary systems with properly aligned energy levels and overlapping absorption among the components hold great promises to further enhance the performance of corresponding binary ones.

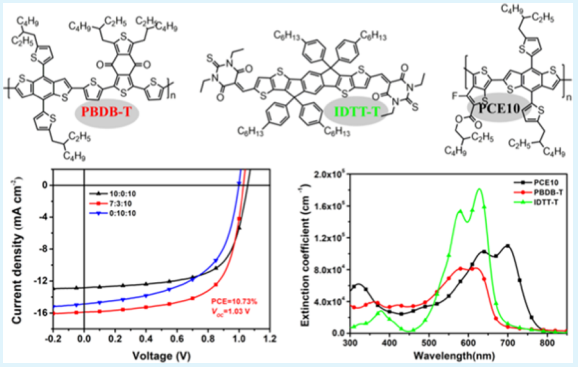

KEYWORDS: *energy transfer, induced crystallization property, molecular mediator, nonfullerene acceptors, ternary solar cell*

INTRODUCTION

Organic solar cells (OSCs) have become an attractive photovoltaic technology on account of the flexibility, low-cost fabrication, and the great potential for high throughput large-area production.[1−3] Device performances have been improved significantly in the past few years owing to the great advancement of new materials, better control of film morphology, and the optimization of device architecture.[4−13] In particular, a recent burst of research interest in nonfullerene acceptors (NFAs) represents the most exciting progress in the field of OSCs. Owing to the greater tunability of optical and electronic properties of NFAs, the power conversion efficiency (PCE) of NFA-based OSC devices has exceeded 15% that is far beyond the most efficient fullerene-based OSC devices.[14−20] However, the disadvantages of intrinsically limited absorption properties of organic photovoltaic materials and inferior film morphology of some binary blend films impede the further improvement of the PCE. The ternary blend strategy exploits a single active layer containing three different components,[21−23] which offers a mix-and-match solution to improve spectral coverage,[24−26] realize the desirable energy-level cascade,[27,28] facilitate exciton separation and charge transport,[29−31] decrease the density of trap states, suppress charge recombination,[32,33] and eventually achieve a high PCE. At the same time, an in-depth understanding of the basic working mechanisms[34,35] that govern the charge dynamics of devices would make it possible to fabricate ternary solar cells with simultaneously enhanced open-circuit voltage (V_{OC}), short-circuit current density (J_{SC}), and fill factor (FF).[36,37]

So far, a lot of novel NFAs with tunable energy levels and excellent photovoltaic performances have been synthesized, providing more choices for fabricating highly efficient ternary OSCs. High-performing NFAs almost unanimously feature a fused-ring core such as dithienothiophen[3,2-*b*]-pyrrolobenzothiadiazole (TPBT),[14,38] dithienothiophen[3,2-*b*]-pyrrolobenzotriazole (BZPT),[39] indacenodithiophene (IDT),[40,41] indacenodithieno[3,2-*b*]thiophene (IDTT),[42,43] or their derivatives. All of these NFA molecules show good solubility in chloroform, chlorobenzene, and even environmentally benign hydrocarbon solvents. Ternary solar cells based on these NFAs have exhibited excellent photovoltaic performance over 14%.[44−47] At the same time, insight into the effect of the third component on the photophysical processes,

Received: December 30, 2019
Accepted: March 17, 2020
Published: March 17, 2020

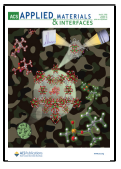

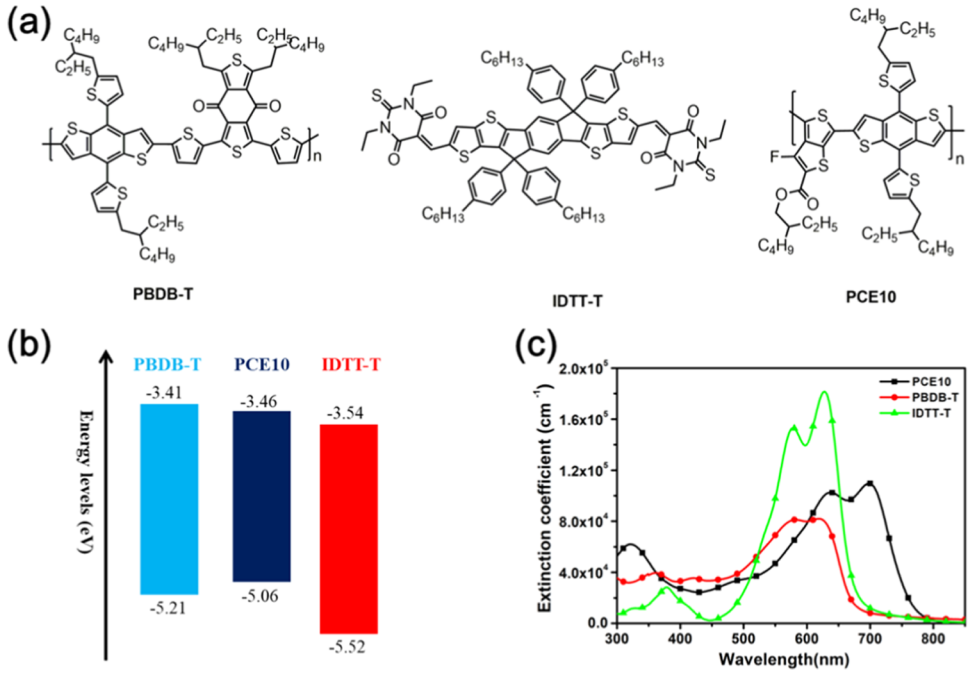

Figure 1. (a) Chemical structures and (b) energy-level diagrams of PBDB-T, IDTT-T, and PCE10; (c) extinction coefficients of PBDB-T, IDTT-T, and PCE10 in the films.

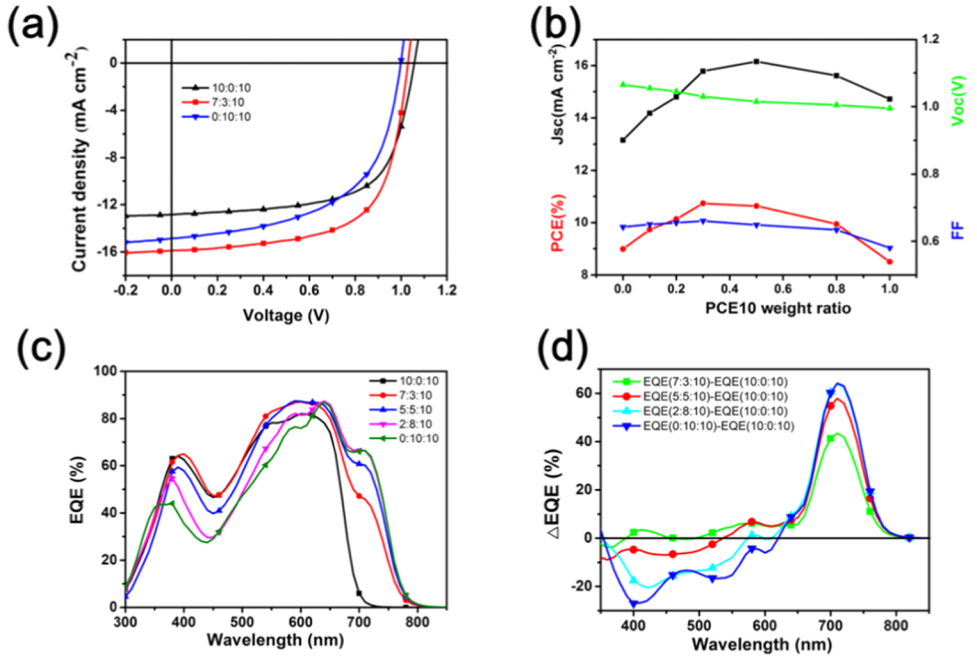

Figure 2. (a) Typical $J-V$ curves of the binary devices and the ternary device with the highest PCE. (b) Plots of J_{SC}, V_{OC}, FF, and PCE at different PCE10 weight ratios. (c) The EQE curves of ternary devices with different PCE10 weight ratios. (d) Difference EQE spectra.

film morphology, and photoelectric conversion process has also been investigated.

Recently, we reported a new A−D−A-structured NFA IDTT-T with a wide band gap, which contains two weakly electron-deficient *N*-ethyl thiabarbituric acid terminal groups and an electron-donating indacenodithienothiophene core. When paired with a polymer donor for fabricating OSCs, the devices showcase a high V_{OC} of 1.01 V, together with an energy loss of 0.57 eV in 9.2% efficiency single-junction NFA OSCs.[48] The device has an attractive V_{OC}, but suffers from relatively low FF and J_{SC}, giving rise to only modest PCE that is less than 10%. Inspired by the ternary strategies, here we report a new kind of ternary OSCs by adding a narrow-band-gap polymer PCE10 as a mediator to the PBDB-T:IDTT-T binary blend system for elevating the FF and J_{SC}. Thanks to the efficient energy transfer, induced crystallization properties, and the improved charge-transfer efficiency, photovoltaic performance of the ternary solar cells is considerably enhanced over the corresponding binary devices, with a PCE enhancement from 8.99 to 10.73%, a J_{SC} increase from 13.15 to 15.78 mA cm^{-2}, and a FF increase from 64.21 to 66.02%.

https://dx.doi.org/10.1021/acsami.9b23516
ACS Appl. Mater. Interfaces 2020, 12, 16387−16393

Table 1. Summary of Device Performance of Ternary Solar Cells at Different Weight Ratios of PCE10

PBDB-T:PCE10:IDTT-T	J_{SC} (mA cm^{-2})	V_{OC} (V)	FF (%)	PCE (%)
10:0:10	13.15 (12.83)[a]	1.065	64.21	8.99[b] (8.66 ± 0.09)[c]
9:1:10	14.18 (13.79)[a]	1.055	65.02	9.73[b] (9.52 ± 0.11)[c]
8:2:10	14.80 (14.43)[a]	1.045	65.48	10.13[b] (9.97 ± 0.14)[c]
7:3:10	15.78 (15.62)[a]	1.030	66.02	10.73[b] (10.53 ± 0.15)[c]
5:5:10	16.15 (15.88)[a]	1.015	64.88	10.63[b] (10.42 ± 0.15)[c]
2:8:10	15.61 (15.17)[a]	1.005	63.40	9.94[b] (9.74 ± 0.13)[c]
0:10:10	14.72 (14.53)[a]	0.995	58.01	8.50[b] (8.23 ± 0.11)[c]

[a]J_{SC} calculated from external quantum efficiency (EQE) curves. [b]The best PCE. [c]Average PCE from 10 devices.

EXPERIMENTAL SECTION

The experimental details are shown in the Supporting Information.

RESULTS AND DISCUSSION

Figure 1a shows the chemical structures of PBDB-T, IDTT-T, and PCE10, and the corresponding energy-level alignment is depicted in Figure 1b. Compared to the pioneering study by Zhan et al. that employed ITIC as the narrow-band-gap NFA for OSCs,[49] weakly electron-withdrawing *N*,*N*′-diethyl thiobarbituric acid (TBA) end groups are employed to replace the strongly electron-accepting cyano indone groups to give a novel wide band-gap NFA IDTT-T. The lowest unoccupied molecular orbital (LUMO) energy level of IDTT-T is −3.51 eV and is significantly higher than that of ITIC, which would contribute to the high V_{OC} in binary and ternary OSC devices. The absorption spectra of the thin films of PBDB-T, IDTT-T, and PCE10 show the lowest-energy peaks at around 620, 627, and 700 nm, with extinction coefficients of 8.15×10^4, 1.81×10^5, and 1.10×10^5 cm^{-1}, respectively (Figure 1c). PCE10 exhibits the onset absorption at around 800 nm, which broadens the photon harvesting range when compared with the PBDB-T:IDTT-T blend film. Therefore, incorporation of PCE10 into the binary mixture could harvest photons more effectively in the spectroscopic region between 670 and 790 nm (Figure S1). Furthermore, PBDB-T and IDTT-T show overlapped absorption between 550 and 650 nm, confirming effective photon harvesting in this energy range. Slightly decreased absorption in the ternary blend films in this region would not lead to a decrease in photocurrent due to the large extinction coefficient. Overall, improved J_{SC} is anticipated on account of the absorption features of such ternary blends.

OSC devices were fabricated based on an inverted structure of indium-tin-oxide (ITO)/sol−gel ZnO/active materials/MoO_3/Al (see the Supporting Information for details of the fabrication process). The representative current density−voltage (*J*−*V*) curves of two binary OSCs and the best-performing ternary solar cell under one standard sun illumination are displayed in Figure 2a, and the main photovoltaic parameters are summarized in Table 1. The optimal PBDB-T:IDTT-T-based binary devices show a PCE of 8.99%, a moderate J_{SC} of 13.15 mA cm^{-2}, and a notably high V_{OC} of 1.065 V, which correlates well with the large gap between the LUMO energy level of IDTT-T and the highest occupied molecular orbital (HOMO) of PBDT-T. The PCE10:IDTT-T-based binary solar cell shows a PCE of 8.50%, a higher J_{SC} of 14.72 mA cm^{-2}, and an inferior FF of 58.01%. For the ternary solar cells, PBDB-T:PCE10 weight ratios are progressively varied, while the overall donor/acceptor ratio is fixed at 1:1. Figure 2b shows that the J_{SC} values of the ternary solar cells increase significantly, which peaks at 50 wt % PCE10. FF values of the devices enhance to 66.02% when 30 wt % PCE10 is employed as the third component and then decrease. Contrary to the trends in J_{SC} and FF variations, V_{OC} is monotonically decreased upon increasing the weight ratio of PCE10. Such V_{OC} dependence on compositions in ternary blend devices indicates that both PBDB-T and PCE10 effectively collect the holes without energy-level pinning. The HOMO level of PCE10 is higher than PBDB-T, thus PCE10 may potentially act as trapping site for holes from PBDB-T. If this occurs, however, the energy level will be pinned to PCE10 and a constant V_{OC} irrelevant to the composition of PCE10 is expected, which contrasts with our observations. The lack of energy-level pinning also corroborates well with the enhanced hole mobility in ternary devices (see discussions later), which supports that PCE10 does not act as hole trapping sites. On the other hand, PCE10 acts as an electron relay station between PBDB-T and IDTT-T due to the cascade-aligned LUMO energy levels (Figure 1c) that facilitate electron transfer.[50] In other words, photoinduced electrons from PBDB-T could transfer to either PCE10 or IDTT-T and the electrons from excited PCE10 to IDTT-T are also effective.

External quantum efficiency (EQE) spectra of the corresponding devices were measured to prove the J_{SC} improvement and confirm the contribution of ternary components to the photocurrent. As shown in Figures 2c and S2, the PBDB-T:IDTT-T-based binary device shows a primary EQE response within the limited range of 500−700 nm, which results in the low integrated current density (J_{int}) of 12.83 mA cm^{-2}. EQE response of the PCE10:IDTT-T-based binary solar cell is mostly in the spectrum range between 500 and 800 nm (calculated J_{int}: 14.53 mA cm^{-2}). The EQE difference is plotted in Figure 2d, showing that EQE response of the ternary solar cell in the range of 700−800 nm is gradually enhanced with the addition of PCE10 from 0 to 100 wt %, which correlates well with the absorption feature of PCE10. The EQE values in the range between 550 and 650 nm are also increased regardless of the slightly decreased absorption intensity when the component of PCE10 is less than 50 wt %. As we know, EQE depends on incident photoabsorption and free charge carrier recombination and EQE values would elevate when the increased free carriers induced by light absorption are large than the decreased free carrier due to the recombination. In this contribution, the absorption property of ternary blend films within the region of 550−650 nm is no longer the limited factor in EQE improvement because of its large extinction coefficient and the enhanced exciton separation and charge carrier collection would be responsible for the increased EQE values. In addition, the J_{SC} values from integrating the EQE spectra are close to those from device measurements (Table 1).

https://dx.doi.org/10.1021/acsami.9b23516
ACS Appl. Mater. Interfaces 2020, 12, 16387−16393

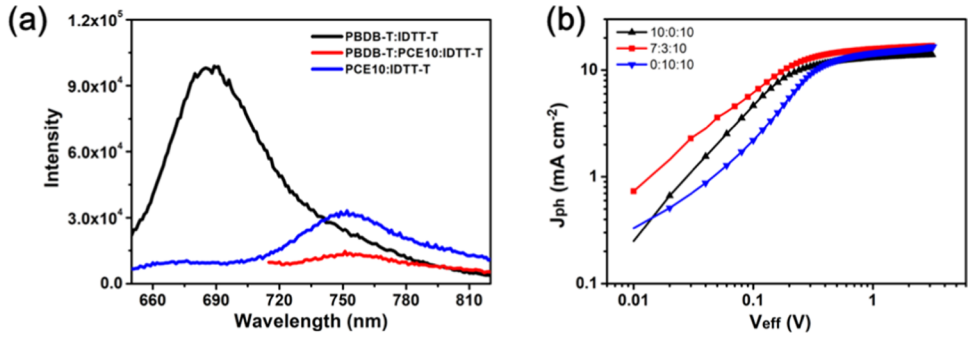

Figure 3. (a) PL spectra of PBDB-T:IDTT-T, PCE10:IDTT-T binary blend films and PBDB-T:PCE10:IDTT-T ternary blend film; (b) J_{ph} versus V_{eff} curves of solar cells with different amounts of PCE10.

To understand the improvement of device performance and related physical processes in the ternary blend systems, steady-state photoluminescence (PL) spectroscopic studies of individual component films and different ternary thin films were performed. As shown in Figure S3, the binary PBDB-T and PCE10 blend film shows PL behavior characteristic of fluorescence resonance energy transfer (FRET). The PL peaks for PBDB-T and PCE10 were at 680 and 760 nm, respectively. For the PBDB-T:PCE10 binary blend film, there is only one maximum peak at the position of 753 nm, which is similar to the PL peak position of PCE10. In addition, the emission peak of PBDB-T shows an obvious overlap with the absorption of PCE10. The efficient nonradiative energy transfer also indicates the well-mixed and close packing (within 10 nm) properties,[51] which is also likely responsible for the high component tolerance. The ternary blend film shows more efficient quenching than corresponding binary blend films (Figure 3a), an indication of the improved charge-transfer process when PCE10 is added as a molecular mediator. Further studies on the charge generation and separation process in ternary devices are carried out by investigating the saturation photocurrent density (J_{sat}) and charge separation probabilities $P(E,T)$.[52] As shown in Figure 3b, the higher photocurrent density (J_{ph}) of ternary devices at a low effective voltage (V_{eff}) indicates more efficient exciton separation and charge collection. The $P(E,T)$ of the devices, calculated based on the J_{ph}/J_{sat} ratio under short-circuit conditions, are 95.9, 96.3, and 94.2% for PBDB-T:PCE10:IDTT-T-based devices at weight ratios of 10:0:10, 7:3:10, and 0:10:10, respectively. The ternary device has the highest $P(E,T)$ value, corresponding to a higher charge dissociation rate that leads to improved J_{SC} and FF. Another parameter, the maximum exciton generation rate (G_{max}), is calculated by the equation $J_{sat} = qLG_{max}$, where q is the elementary charge and L is the film thickness. For PBDB-T:PCE10:IDTT-T-based devices at weight ratios of 10:0:10, 7:3:10, and 0:10:10, the corresponding G_{max} are 8.57×10^{27} m^{-3} s^{-1} (J_{sat} = 137.1 A m^{-2}), 1.02×10^{28} m^{-3} s^{-1} (J_{sat} = 163.8 A m^{-2}), and 9.76×10^{27} m^{-3} s^{-1} (J_{sat} = 156.1 A m^{-2}), respectively. The highest G_{max} in the ternary cell indicates that more excitons are generated after adding PCE10 as the third component, which is also associated with broader absorption, efficient FRET between PBDB-T and PCE10, and charge transfer in the ternary blend system. We also investigated the carrier-transport property by using the space charge limited current (SCLC) method (see the Supporting Information and Figures S4 and S5 for details of device fabrication and measurement). The hole and electron mobilities are 5.01×10^{-4} and 2.52×10^{-4} cm^2 V^{-1} s^{-1} for the binary PBDB-T:IDTT-T-based device and 5.32×10^{-4} and 2.87×10^{-4} cm^2 V^{-1} s^{-1} for the best ternary device, respectively. Both hole and electron mobilities are increased in the ternary device, corroborating well with the enhanced FF and J_{SC} in such solar cells.

Transmission electron microscopy (TEM) studies reveal that (Figure 4) there is no obvious phase separation in the PCE10:IDTT-T binary blend film, which is not ideal for charge transportation and leads to inferior FF of 58.01%. For the PBDB-T:IDTT-T binary blend film, some degree of nanofibrillar phase separation emerges but is not clearly defined. The fiber-like bicontinuous charge transportation networks are more obvious in PBDB-T:PCE10:IDTT-T-based ternary blend films at weight ratios of 7:3:10, 5:5:10, which is conducive to balancing charge generation and transportation and therefore lead to higher J_{SC} and FF. The width for the nanofibers is around 15 nm in the 7:3:10 ternary thin film, in accordance with the ideal size for nanophase segregations.

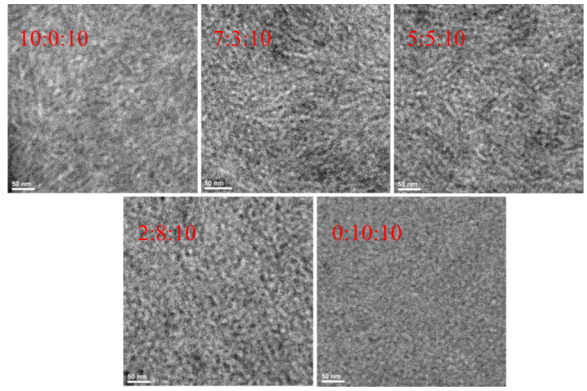

Figure 4. TEM images of PBDB-T:PCE10:IDTT-T blend films at different weight ratios.

More insight into the effect of PCE10 on the ternary blend film morphology is obtained from the grazing incidence wide-angle X-ray scattering (GIWAXS) experiment. The scattering patterns of three pure films and the ternary blend films with different weight ratios of PCE10 are shown in Figures S6 and 5a. The GIWAXS patterns of PBDB-T and PCE10 indicate that these two electron donors form crystallites with a preferred face-on orientation. X-ray scattering arcs of IDTT-T were observed along both in-plane and out-of-plane (OOP) directions, suggesting the random arrangement of crystallites with no preferred orientation. The corresponding OOP line-cut profiles (Figure 5b and S7) display (100), (200), and

https://dx.doi.org/10.1021/acsami.9b23516
ACS Appl. Mater. Interfaces 2020, 12, 16387−16393

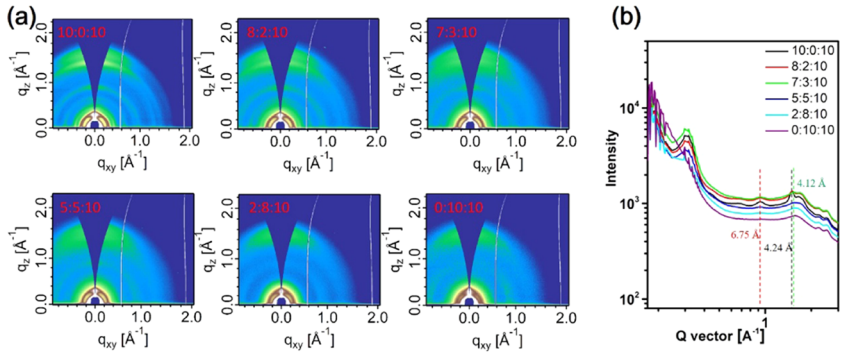

Figure 5. (a) GIWAXS patterns and (b) OOP line cuts of PBDB-T:PCE10:IDTT-T blend films at different weight ratios.

(300) peaks at 0.31, 0.62, and 0.93 A^{-1} and (010) peak at 1.71 A^{-1} in the OOP direction, indicating lamellar stacking of PBDB-T main chains via $\pi-\pi$ stacking. PCE10 also shows an (010) peak at 1.59 A^{-1} with a d spacing of 3.95 Å. For the ternary blend films with higher PBDT-T compositions, the OOP line cut shows the third-order reflection peak at 0.93 A^{-1}, arising from the lamellar packing of PBDT-T, as well as two π-stacking peaks that are associated with PBDT-T and IDTT-T, respectively. The high-order peak at 0.93 A^{-1} disappeared for the PBDB-T:PCE10:IDTT-T blends at weight ratios of 5:5:10, 2:8:10, and 0:10:10, together with the blending of the two π-stacking peaks into indistinguishable reflection, which may suggest that the suppressed lamellar stacking correlates to the decreased FF and device performance. Furthermore, closer $\pi-\pi$ stacking of the conjugated backbone was observed when the weight ratio of PCE10 increased from 0 to 30 wt %. The d spacing of one of the π-stacking peaks decreased from 4.24 Å for the 10:0:10 blend to 4.12 Å for the 7:3:10 blend film. The tighter packing would facilitate carrier transport and suppress charge recombination, which also correlates well with the enhanced carrier mobility measured by the SCLC method.

CONCLUSIONS

Our work have demonstrated that the PCE of PBDB-T:IDTT-T-based solar cells could be enhanced by adding a narrow-band-gap polymer PCE10 as the third component. The extended absorption, efficient FRET, enhanced charge dissociation, and tighter molecular packing of the ternary blend films in this contribution increase the J_{SC} from 13.15 to 16.15 mA cm^{-2}. The optimized ternary blend solar cells deliver a champion PCE of 10.73% with a J_{SC} of 15.78 mA cm^{-2}, a FF of 66.02%, and a high V_{OC} of 1.03 V. It also represents a rare example for the ternary solar cell device with the PCE larger than 10% together with a V_{OC} greater than 1 V. In addition, the ternary OSC devices exhibit over 10% PCEs at a range of compositions as a result of good component miscibility and favorable film morphology within a certain composition window. This work proves that efficient energy transfer and induced crystallization can improve the performance of ternary devices. More comprehensive studies associated with FRET and crystallization to improve the photovoltaic properties are currently ongoing in our lab.

ASSOCIATED CONTENT

Supporting Information

The Supporting Information is available free of charge at https://pubs.acs.org/doi/10.1021/acsami.9b23516.

Absorption spectra of ternary blend films with different weight ratios of PCE10 (Figure S1); EQE curves of ternary solar cell devices based on different weight ratios of PCE10 (Figure S2); photoluminescence spectra of pristine PBDB-T, PCE10, IDTT-T, and PBDB-T:PCE10 blend films with a weight ratio of 1:1 (Figure S3); hole and electron mobilities of the optimal PBDB-T:PCE10:IDTT-T-based device and corresponding binary device (Table S1) (PDF)

AUTHOR INFORMATION

Corresponding Authors

Yonggang Min − *School of Materials and Energy, Guangdong University of Technology, Guangzhou 510006, China;* orcid.org/0000-0001-9215-8742; Email: ygmin@gdut.edu.cn

Yi Liu − *The Molecular Foundry, Lawrence Berkeley National Lab, Berkeley, California 94720, United States;* orcid.org/0000-0002-3954-6102; Email: yliu@lbl.gov

Authors

Liangang Xiao − *School of Materials and Energy, Guangdong University of Technology, Guangzhou 510006, China; The Molecular Foundry, Lawrence Berkeley National Lab, Berkeley, California 94720, United States;* orcid.org/0000-0002-7901-9884

Haiyan Mao − *College of Materials Science and Engineering, Nanjing Forestry University, Nanjing 210037, China; Department of Chemical and Biomolecular Engineering, University of California Berkeley, Berkeley, California 94720, United States*

Zhengdong Li − *School of Materials and Energy, Guangdong University of Technology, Guangzhou 510006, China*

Cong Yan − *School of Materials and Energy, Guangdong University of Technology, Guangzhou 510006, China*

Jia Liu − *School of Materials and Energy, Guangdong University of Technology, Guangzhou 510006, China*

Yidong Liu − *School of Materials and Energy, Guangdong University of Technology, Guangzhou 510006, China*

Jeffrey A. Reimer − *Department of Chemical and Biomolecular Engineering, University of California Berkeley, Berkeley, California 94720, United States;* orcid.org/0000-0002-4191-3725

Complete contact information is available at: https://pubs.acs.org/10.1021/acsami.9b23516

Author Contributions

[⊥]L.X. and H.M. contributed equally to this work.

https://dx.doi.org/10.1021/acsami.9b23516
ACS Appl. Mater. Interfaces 2020, 12, 16387−16393

Notes

The authors declare no competing financial interest.

■ ACKNOWLEDGMENTS

L.X. thanks the financial support from the National Natural Science Foundation of China (51903057) and the Hundred Young Talent Program of the Guangdong University of Technology (220413291). Y.M. thanks the support from Guangdong Innovative and Entrepreneurial Research Team Program (No. 2016ZT06C412). Part of this work was performed as a user project at the Molecular Foundry, and the GIWAXS data was collected at beamline 7.3.3 at the Advanced Light Source (ALS) at Lawrence Berkeley National Laboratory, both supported by the DOE, Office of Science, and Office of Basic Energy Sciences. Teresa Chen and Liana M. Klivansky are acknowledged for their help with device fabrication, Dr. Bo He and Dr. Matthew Kolaczkowski for help with material synthesis, and Dr. Chenhui Zhu for beamline support.

■ REFERENCES

(1) Yu, G.; Gao, J.; Hummelen, J. C.; Wudl, F.; Heeger, A. J. Polymer Photovoltaic Cells: Enhanced Efficiencies via a Network of Internal Donor-acceptor Heterojunctions. *Science* **1995**, *270*, 1789−1791.

(2) Krebs, F. C.; Espinosa, N.; Hosel, M.; Sondergaard, R. R.; Jorgensen, M. 25th Anniversary Article: Rise to Power - OPV-Based Solar Parks. *Adv. Mater.* **2014**, *26*, 29−39.

(3) Shaheen, S. E.; Brabec, C. J.; Sariciftci, N. S.; Padinger, F.; Fromherz, T.; Hummelen, J. C. 2.5% Efficient Organic Plastic Solar Cells. *Appl. Phys. Lett.* **2001**, *78*, 841−843.

(4) Xiao, L. G.; Li, Z. D.; Hu, Q.; Liu, Y. W.; Zhong, W. K.; Mei, X. L.; Russell, T. P.; Liu, Y.; Min, Y.; Peng, X. B.; Cao, Y. Improving the Efficiencies of Small Molecule Solar Cells by Solvent Vapor Annealing to Enhance J-aggregation. *J. Mater. Chem. C* **2019**, *7*, 9618−9624.

(5) Hoppe, H.; Sariciftci, N. S. Morphology of Polymer/fullerene Bulk Heterojunction Solar Cells. *J. Mater. Chem.* **2006**, *16*, 45−61.

(6) He, Z. C.; Zhong, C. M.; Su, S. J.; Xu, M.; Wu, H. B.; Cao, Y. Enhanced Power-conversion Efficiency in Polymer Solar Cells Ssing an Inverted Device Structure. *Nat. Photonics* **2012**, *6*, 591−595.

(7) Sun, Y. M.; Seo, J. H.; Takacs, C. J.; Seifter, J.; Heeger, A. J. Inverted Polymer Solar Cells Integrated with a Low-Temperature-Annealed Sol-Gel-Derived ZnO Film as an Electron Transport Layer. *Adv. Mater.* **2011**, *23*, 1679−1683.

(8) Liao, S. H.; Jhuo, H. J.; Cheng, Y. S.; Chen, S. A. Fullerene Derivative-Doped Zinc Oxide Nanofilm as the Cathode of Inverted Polymer Solar Cells with Low-Bandgap Polymer (PTB7-Th) for High Performance. *Adv. Mater.* **2013**, *25*, 4766−4771.

(9) Zhao, W. C.; Qian, D. P.; Zhang, S. Q.; Li, S. S.; Inganas, O.; Gao, F.; Hou, J. H. Fullerene-Free Polymer Solar Cells with over 11% Efficiency and Excellent Thermal Stability. *Adv. Mater.* **2016**, *28*, 4734−4739.

(10) Yan, C. Q.; Barlow, S.; Wang, Z. H.; Yan, H.; Jen, A. K. Y.; Marder, S. R.; Zhan, X. W. Non-fullerene Acceptors for Organic Solar Cells. *Nat. Rev. Mater.* **2018**, *3*, 18003−18021.

(11) Meng, L. X.; Zhang, Y. M.; Wan, X. J.; Li, C. X.; Zhang, X.; Wang, Y. B.; Ke, X.; Xiao, Z.; Ding, L. M.; Xia, R. X.; Yip, H. L.; Cao, Y.; Chen, Y. S. Organic and Solution-processed Tandem Solar Cells with 17.3% Efficiency. *Science* **2018**, *361*, 1094−1098.

(12) Xiao, L. G.; Lai, T. Q.; Liu, X.; Liu, F.; Russell, T. P.; Liu, Y.; Huang, F.; Peng, X. B.; Cao, Y. A Low-bandgap Dimeric Porphyrin Molecule for 10% Efficiency Solar Cells with Small Photon Energy Loss. *J. Mater. Chem. A* **2018**, *6*, 18469−18478.

(13) Chen, H.; Hu, D.; Yang, Q.; Gao, J.; Fu, J.; Yang, K.; He, H.; Chen, S.; Kan, Z.; Duan, T.; Yang, C.; Ouyang, J.; Xiao, Z.; Sun, K.; Lu, S. All-Small-Molecule Organic Solar Cells with an Ordered Liquid Crystalline Donor. *Joule* **2019**, *3*, No. 3034.

(14) Yuan, J.; Zhang, Y.; Zhou, L.; Zhang, G.; Yip, H.-L.; Lau, T.-K.; Lu, X.; Zhu, C.; Peng, H.; Johnson, P. A. Single-junction Organic Solar Cell with over 15% Efficiency Using Fused-ring Acceptor with Electron-deficient Core. *Joule* **2019**, *3*, 1140−1151.

(15) Sun, H.; Liu, T.; Yu, J.; Lau, T.-K.; Zhang, G.; Zhang, Y.; Su, M.; Tang, Y.; Ma, R.; Liu, B. A Monothiophene Unit Incorporating both Fluoro and Ester Substitution Enabling High-performance Donor Polymers for Non-fullerene Solar Cells with 16.4% Efficiency. *Energy Environ. Sci.* **2019**, *12*, No. 3328.

(16) Cui, Y.; Yao, H. F.; Zhang, J. Q.; Zhang, T.; Wang, Y. M.; Hong, L.; Xian, K. H.; Xu, B. W.; Zhang, S. Q.; Peng, J.; Wei, Z. X.; Gao, F.; Hou, J. H. Over 16% Efficiency Organic Photovoltaic Cells Enabled by a Chlorinated Acceptor with Increased Open-circuit Voltages. *Nat. Commun.* **2019**, *10*, No. 2515.

(17) Fan, B. B.; Zhang, D. F.; Li, M. J.; Zhong, W. K.; Zeng, Z. M. Y.; Ying, L.; Huang, F.; Cao, Y. Achieving over 16% Efficiency for Single-junction Organic Solar Cells. *Sci. China: Chem.* **2019**, *62*, 746−752.

(18) Xu, X.; Feng, K.; Bi, Z.; Ma, W.; Zhang, G.; Peng, Q. Single-Junction Polymer Solar Cells with 16.35% Efficiency Enabled by a Platinum(II) Complexation Strategy. *Adv. Mater.* **2019**, *31*, No. 1901872.

(19) Zhou, Z. C.; Liu, W. R.; Zhou, G. Q.; Zhang, M.; Qian, D. P.; Zhang, J. Y.; Chen, S. S.; Xu, S. J.; Yang, C. D.; Gao, F.; Zhu, H. M.; Liu, F.; Zhu, X. Z. Subtle Molecular Tailoring Induces Significant Morphology Optimization Enabling over 16% Efficiency Organic Solar Cells with Efficient Charge Generation. *Adv. Mater.* **2019**, *32*, No. 1906324.

(20) Cui, Y.; Yao, H.; Hong, L.; Zhang, T.; Tang, Y.; Lin, B.; Xian, K.; Gao, B.; An, C.; Bi, P. 17% Efficiency Organic Photovoltaic Cell with Superior Processability. *Natl. Sci. Rev.* **2019**, No. nwz200.

(21) Ameri, T.; Khoram, P.; Min, J.; Brabec, C. J. Organic Ternary Solar Cells: A Review. *Adv. Mater.* **2013**, *25*, 4245−4266.

(22) Gasparini, N.; Salleo, A.; McCulloch, I.; Baran, D. The Role of the Third Component in Ternary Organic Solar Cells. *Nat. Rev. Mater.* **2019**, *4*, 229−242.

(23) An, Q. S.; Zhang, F. J.; Zhang, J.; Tang, W. H.; Deng, Z. B.; Hu, B. Versatile Ternary Organic Solar Cells: a Critical Review. *Energy Environ. Sci.* **2016**, *9*, 281−322.

(24) Xiao, L. G.; Gao, K.; Zhang, Y. D.; Chen, X. B.; Hou, L. T.; Cao, Y.; Peng, X. B. A Complementary Absorption Small Molecule for Efficient Ternary Organic Solar Cells. *J. Mater. Chem. A* **2016**, *4*, 5288−5293.

(25) Xiao, Z.; Jia, X.; Ding, L. M. Ternary Organic Solar Cells Offer 14% Power Conversion Efficiency. *Sci. Bull.* **2017**, *62*, 1562−1564.

(26) Piradi, V.; Xu, X.; Wang, Z.; Ali, J.; Peng, Q.; Liu, F.; Zhu, X. Panchromatic Ternary Organic Solar Cells with Porphyrin Dimers and Absorption-Complementary Benzodithiophene-based Small Molecules. *ACS Appl. Mater. Interfaces* **2019**, *11*, 6283−6291.

(27) Lu, L. Y.; Xu, T.; Chen, W.; Landry, E. S.; Yui, L. P. Ternary Blend Polymer Solar Cells with Enhanced Power Conversion Efficiency. *Nat. Photonics* **2014**, *8*, 716−722.

(28) Jiang, W. G.; Yu, R. N.; Liu, Z. Y.; Peng, R. X.; Mi, D. B.; Hong, L.; Wei, Q.; Hou, J. H.; Kuang, Y. B.; Ge, Z. Y. Ternary Nonfullerene Polymer Solar Cells with 12.16% Efficiency by Introducing One Acceptor with Cascading Energy Level and Complementary Absorption. *Adv. Mater.* **2018**, *30*, No. 1703005.

(29) Xiao, L. G.; Liang, T. X.; Gao, K.; Lai, T. Q.; Chen, X. B.; Liu, F.; Russell, T. P.; Huang, F.; Peng, X. B.; Cao, Y. Ternary Solar Cells Based on Two Small Molecule Donors with Same Conjugated Backbone: The Role of Good Miscibility and Hole Relay Process. *ACS Appl. Mater. Interfaces* **2017**, *9*, 29917−29923.

(30) Cheng, H. W.; Zhang, H. T.; Lin, Y. C.; She, N. Z.; Wang, R.; Chen, C. H.; Yuan, J.; Tsao, C. S.; Yabushita, A.; Zou, Y. P.; Gao, F.; Cheng, P.; Wei, K. H.; Yang, Y. Realizing Efficient Charge/Energy Transfer and Charge Extraction in Fullerene-Free Organic Photovoltaics via a Versatile Third Component. *Nano Lett.* **2019**, *19*, 5053−5061.

https://dx.doi.org/10.1021/acsami.9b23516
ACS Appl. Mater. Interfaces 2020, 12, 16387−16393

(31) Zhang, M.; Zhang, Z.; Wang, J.; An, Q.; Peng, H.; Tang, W.; Zhang, F. 13.26% Efficiency Polymer Solar Cells by Optimizing Photogenerated Exciton Distribution and Phase Separation with the Third Component. *Sol. RRL* **2019**, *3*, No. 1900269.
(32) Gasparini, N.; Jiao, X.; Heumueller, T.; Baran, D.; Matt, G. J.; Fladischer, S.; Spiecker, E.; Ade, H.; Brabec, C. J.; Ameri, T. Designing Ternary Blend Bulk Heterojunction Solar Cells with Reduced Carrier Recombination and a Fill Factor of 77%. *Nat. Energy* **2016**, *1*, 16118−16122.
(33) Zhang, M.; Gao, W.; Zhang, F. J.; Mi, Y.; Wang, W. B.; An, Q. S.; Wang, J.; Ma, X. L.; Miao, J. L.; Hu, Z. H.; Liu, X. F.; Zhang, J.; Yang, C. L. Efficient Ternary Non-fullerene Polymer Solar Cells with PCE of 11.92% and FF of 76.5%. *Energy Environ. Sci.* **2018**, *11*, 841−849.
(34) Wang, Z.; Zhu, X. W.; Zhang, J. Q.; Lu, K.; Fang, J.; Zhang, Y. J.; Wang, Z. Y.; Zhu, L. Y.; Ma, W.; Shuai, Z. G.; Wei, Z. X. From Alloy-Like to Cascade Blended Structure: Designing High-Performance All-Small-Molecule Ternary Solar Cells. *J. Am. Chem. Soc.* **2018**, *140*, 1549−1556.
(35) Bi, P. Q.; Hall, C. R.; Yin, H.; So, S. K.; Smith, T. A.; Ghiggino, K. P.; Hao, X. T. Resolving the Mechanisms of Photocurrent Improvement in Ternary Organic Solar Cells. *J. Phys. Chem. C* **2019**, *123*, 18294−18302.
(36) Xiao, L.; He, B.; Hu, Q.; Maserati, L.; Zhao, Y.; Yang, B.; Kolaczkowski, M. A.; Anderson, C. L.; Borys, N. J.; Klivansky, L. M. Multiple Roles of a Non-fullerene Acceptor Contribute Synergistically for High-efficiency Ternary Organic Photovoltaics. *Joule* **2018**, *2*, 2154−2166.
(37) Pan, M.-A.; Lau, T.-K.; Tang, Y.; Wu, Y.-C.; Liu, T.; Li, K.; Chen, M.-C.; Lu, X.; Ma, W.; Zhan, C. 16.7%-efficiency Ternary Blended Organic Photovoltaic Cells with PCBM as the Acceptor Additive to Increase the Open-circuit Voltage and Phase Purity. *J. Mater. Chem. A.* **2019**, *7*, 20713−20722.
(38) Yuan, J.; Zhang, Y. Q.; Zhou, L. Y.; Zhang, C. J.; Lau, T. K.; Zhang, G. C.; Lu, X. H.; Yip, H. L.; So, S. K.; Beaupre, S.; Mainville, M.; Johnson, P. A.; Leclerc, M.; Chen, H. G.; Peng, H. J.; Li, Y. F.; Zou, Y. P. Fused Benzothiadiazole: A Building Block for n-Type Organic Acceptor to Achieve High-Performance Organic Solar Cells. *Adv. Mater.* **2019**, *31*, No. 1807577.
(39) Yuan, J.; Huang, T. Y.; Cheng, P.; Zou, Y. P.; Zhang, H. T.; Yang, J. L.; Chang, S. Y.; Zhang, Z. Z.; Huang, W. C.; Wang, R.; Meng, D.; Gao, F.; Yang, Y. Enabling Low Voltage Losses and High Photocurrent in Fullerene-free Organic Photovoltaics. *Nat. Commun.* **2019**, *10*, No. 570.
(40) Feng, S. Y.; Zhang, C. E.; Liu, Y. H.; Bi, Z. Z.; Zhang, Z.; Xu, X. J.; Ma, W.; Bo, Z. S. Fused-Ring Acceptors with Asymmetric Side Chains for High-Performance Thick-Film Organic Solar Cells. *Adv. Mater.* **2017**, *29*, No. 1703527.
(41) Wu, Y.; Bai, H. T.; Wang, Z. Y.; Cheng, P.; Zhu, S. Y.; Wang, Y. F.; Ma, W.; Zhan, X. W. A Planar Electron Acceptor for Efficient Polymer Solar Cells. *Energy Environ. Sci.* **2015**, *8*, 3215−3221.
(42) Zhao, W. C.; Li, S. S.; Yao, H. F.; Zhang, S. Q.; Zhang, Y.; Yang, B.; Hou, J. H. Molecular Optimization Enables over 13% Efficiency in Organic Solar Cells. *J. Am. Chem. Soc.* **2017**, *139*, 7148−7151.
(43) Fei, Z. P.; Eisner, F. D.; Jiao, X. C.; Azzouzi, M.; Rohr, J. A.; Han, Y.; Shahid, M.; Chesman, A. S. R.; Easton, C. D.; McNeill, C. R.; Anthopoulos, T. D.; Nelson, J.; Heeney, M. An Alkylated Indacenodithieno[3,2-b] thiophene-Based Nonfullerene Acceptor with High Crystallinity Exhibiting Single Junction Solar Cell Efficiencies Greater than 13% with Low Voltage Losses. *Adv. Mater.* **2018**, *30*, No. 1705209.
(44) Li, K.; Wu, Y.; Tang, Y.; Pan, M.-A.; Ma, W.; Fu, H.; Zhan, C.; Yao, J. Ternary Blended Fullerene-Free Polymer Solar Cells with 16.5% Efficiency Enabled with a Higher-LUMO-Level Acceptor to Improve Film Morphology. *Adv. Energy Mater.* **2019**, *9*, No. 1901728.
(45) Ma, Y.; Zhou, X.; Cai, D.; Tu, Q.; Ma, W.; Zheng, Q. A Minimal Benzo[c][1,2,5]thiadiazole-based Electron Acceptor as a Third Component Material for Ternary Polymer Solar Cells with Efficiencies Exceeding 16.0%. *Mater. Horiz.* **2019**, *7*, 117−124.
(46) Liu, T.; Luo, Z. H.; Fan, Q. P.; Zhang, G. Y.; Zhang, L.; Gao, W.; Guo, X.; Ma, W.; Zhang, M. J.; Yang, C. L.; Li, Y. F.; Yan, H. Use of two Structurally Similar Small Molecular Acceptors Enabling Ternary Organic Solar Cells with High Efficiencies and Fill Factors. *Energy Environ. Sci.* **2018**, *11*, 3275−3282.
(47) Jiang, K.; Wei, Q.; Lai, J. Y. L.; Peng, Z.; Kim, H. K.; Yuan, J.; Ye, L.; Ade, H.; Zou, Y.; Yan, H. Alkyl Chain Tuning of Small Molecule Acceptors for Efficient Organic Solar Cells. *Joule* **2019**, *3*, 3020−3033.
(48) He, B.; Yang, B.; Kolaczkowski, M. A.; Anderson, C. A.; Klivansky, L. M.; Chen, T. L.; Brady, M. A.; Liu, Y. Molecular Engineering for Large Open-Circuit Voltage and Low Energy Loss in Around 10% Non-fullerene Organic Photovoltaics. *ACS Energy Lett.* **2018**, *3*, 1028−1035.
(49) Lin, Y. Z.; Wang, J. Y.; Zhang, Z. G.; Bai, H. T.; Li, Y. F.; Zhu, D. B.; Zhan, X. W. An Electron Acceptor Challenging Fullerenes for Efficient Polymer Solar Cells. *Adv. Mater.* **2015**, *27*, 1170−1174.
(50) Street, R. A.; Davies, D.; Khlyabich, P. P.; Burkhart, B.; Thompson, B. C. Origin of the Tunable Open-Circuit Voltage in Ternary Blend Bulk Heterojunction Organic Solar Cells. *J. Am. Chem. Soc.* **2013**, *135*, 986−989.
(51) Sapsford, K. E.; Berti, L.; Medintz, I. L. Materials for Fluorescence Resonance Energy Transfer Analysis: Beyond Traditional Donor-acceptor Combinations. *Angew. Chem., Int. Ed.* **2006**, *45*, 4562−4588.
(52) Blom, P. W. M.; Mihailetchi, V. D.; Koster, L. J. A.; Markov, D. E. Device Physics of Polymer: Fullerene Bulk Heterojunction Solar Cells. *Adv. Mater.* **2007**, *19*, 1551−1566.

https://dx.doi.org/10.1021/acsami.9b23516
ACS Appl. Mater. Interfaces 2020, 12, 16387−16393